Materials Research Bulletin 50 (2014) 392–398

Contents lists available at ScienceDirect

Materials Research Bulletin

journal homepage: www.elsevier.com/locate/matresbu

A novel acrylic prepolymer/methacrylate modified nano-SiO_2 composite used for negative photoresist

Yan Yuan *, Ning Chen, Ren Liu, Shengwen Zhang, Xiaoya Liu *

The Key Laboratory of Food Colloids and Biotechnology, Ministry of Education, School of Chemical and Material Engineering, Jiangnan University, Wuxi 214122, PR China

ARTICLE INFO

Article history:
Received 18 April 2013
Received in revised form 28 October 2013
Accepted 5 November 2013
Available online 12 November 2013

Keywords:
A. Composites
A. Electronic materials
B. Chemical synthesis

ABSTRACT

A novel nanocomposite consisting of methacrylate modified nano-SiO_2 (SiO_2MA) and acrylic prepolymer (G-ACP) was found a potential candidate as a negative photoresist. The SiO_2MA was synthesized from glycidyl methacrylate (GMA), 3-aminpropyltriethoxysilane (KH550) and a pre-synthesized nano-SiO_2 through the sol–gel process. G-ACP was synthesized through radical polymerization of five monomers, followed by grafting with carboxyl and methacrylate group. The molecular structures of monomers and polymers were characterized by FT-IR and ^{1}H NMR spectroscopy. Finally, SiO_2MA was added into G-ACP in different contents and treated with a standard thermal and UV-exposure process to obtain a series of cured organic–inorganic nanocomposite photoresists. The formed nanocomposite photoresists exhibited improved photosensitivity and had a low $D_n^{0.5}$ of 26.8 mJ cm^{-2} with 13.7 wt% SiO_2MA. Moreover, the thermal and mechanical properties also showed great enhancement while all of the photoresists had a nice line pattern of less than 25 μm.

1. Introduction

Recent years, negative photoresists have been extensively utilized in industry fields for microelectronics, printed circuit boards, liquid crystal displays, nano- imprints and so on [1–7]. Commonly, a large number of negative photoresists contain acrylic prepolymer as the most important component for their high photo-curing reactivity [8,9].

However, photoresists with single organic phase have some problems in patterns transfer process due to low photosensitivity and large thermal expansion coefficient of polymers, resulting in low pattern resolution. Therefore, organic–inorganic nanocomposites have been introduced into photoresists to bring in the advantages of inorganic materials, such as enhanced thermal stability, higher mechanical properties and low thermal expansion coefficient [10–14]. The use of silica particles as inorganic component has drawn more and more attention because of their transparency and adhesion properties. Jiguet and co-workers prepared a nanocomposite consisting of SU-8 resin and nano-silica particles, which possessed higher photosensitivity and less cracks than pure SU-8 photoresist [15].

Also some research focus on polyhedral oligomeric silsesquioxanes (POSS)-based photoresist [16–19]. Silsesquioxane refers a term of matters with the empirical formula of $R_nSi_nO_{1.5n-x}(OH)_{2x}$, which can form ladder, cage-like or polymeric structures [20]. Lin [16] and co-workers synthesized a series of photoresists with methacrylate copolymers containing POSS via the free radical copolymerization. The sensitivity ($D_n^{0.5}$) of the photoresist decreased as the content of POSS increased, from 71.8 mJ cm^{-2} to 10.8 mJ cm^{-2} corresponding to a POSS content of 0–35.5 wt%, respectively. Otherwise, the photopolymerization rate has been improved significantly with the increase of the POSS content, as well as the glass transition temperature (T_g). However, the complicated and time-consuming procedure in the synthesis of POSS limits its application in laboratory research [21,22].

Therefore, the nano-silica sol made from tetraethoxysilane (TEOS) instead of POSS via sol–gel process has been widely reported in recent research [23,24]. The sol–gel process is a wet-chemical technology that is broadly used in the synthesis of glassy or ceramic materials at low temperatures [25–27]. The typical process is consecutive hydrolysis and condensation of an alkoxysilane to form silicone oxides in an aqueous or alcohol solution. Lin [26] and co-workers prepared a negative organic–inorganic photoresist with an acrylic resin and nano-silica. Higher thermal decomposition temperature and T_g were obtained with the increase of silica content, whereas the thermal expansion coefficient decreased. However, the photosensitivity has not

* Corresponding authors. Tel.: +86 510 85917019; fax: +86 510 85917763.
E-mail addresses: yuanyan@jiangnan.edu.cn (Y. Yuan), lxy@jiangnan.edu.cn (X. Liu).

0025-5408/$ – see front matter © 2013 Elsevier Ltd. All rights reserved.
http://dx.doi.org/10.1016/j.materresbull.2013.11.024

shown great improvement due to less acrylate double bonds caused by nano-silica in the resin.

Therefore a methacrylate modified nano-SiO_2 (SiO_2MA) was synthesized and incorporated into an acrylic copolymer (G-ACP), which gave a series of organic–inorganic photoresists via cross-linking reaction of double bonds in acrylate groups from both SiO_2MA and G-ACP. Firstly, five kinds of monomers, including styrene (St), butyl acrylate (BA), methyl methacrylate (MMA), hydroxyethyl acrylate (HEA) and acrylic acid (AA), were copolymerized by free radical polymerization to prepare copolymer (ACP). Then tetrahydrophthalic anhydride (THPA) was added into ACP to introduce carboxylic acid group to the polymer structure (S-ACP). And S-ACP was reacted with glycidyl methacrylate (GMA), which gave an acrylic prepolymer (G-ACP). Secondly, GMA was ring-opened by silane coupling agent 3-aminpropyltriethoxysilane (KH550) to obtain precursor modified methacrylate (KHMA), followed by reaction with pre-synthesized nano-SiO_2 through sol–gel process. Thus, the nano-additive, SiO_2MA, was synthesized. Finally, SiO_2MA was blended with G-ACP in different contents in the presence of photoinitiator and acrylic monomer. Afterwards, the mixtures underwent a standard thermal and UV-exposure process, forming a series of cured organic–inorganic nanocomposites photoresists. The photosensitivity, thermal stability, mechanical properties and resolution were all examined in details.

2. Experimental

2.1. Materials

Styrene (St), butyl acrylate (BA), methyl methacrylate (MMA), hydroxyethyl acrylate (HEA), acrylic acid (AA), tetrahydrophthalic anhydride (THPA), glycidyl methacrylate (GMA), tripropylene glycol diacrylate (TPGDA) and propylene glycol methylether acetate (PMA) were all supplied by Jiangsu Kuangxin Photosensitivity New-material Stock Co., Ltd. (Wuxi, China). Triphenylphosphine (TPP), 2,2′-azobisisobutyronitrile (AIBN), hydroquinone monomethylether (MEHQ), hydroquinone (HQ), 2-mercaptoethanol (2-ME), methanol, ethanol, methyl ethyl ketone (MEK) and ammonium hydroxide ($NH_3{\cdot}H_2O$, 37%) were purchased from Sinopharm Chemical Reagent Co., Ltd. (Shanghai, China). Isopropyl thioxanthone (ITX) and 2-methyl-1-[4-(methylthio)phenyl]-2-(4-morpholinyl)-1-propanon (Irgacure 907) were supplied by Ciba-Geigy Co. (USA). 3-Aminpropyltriethoxysilane (KH550) was purchased from Nanjing Yudeheng Fine Chemical Co. (Nanjing, China). All materials were used as received except AIBN, which should be recrystallized before use.

2.2. Measurements

The Fourier transfer infrared (FT-IR) spectra were collected using an ABB BOMEN FTLA 2000-104 spectrometer with a KBr disk. The Proton Nuclear Magnetic Resonance (^{1}H NMR) spectra were collected with a Bruker Avance Digital 400 MHz spectrometer using tetramethylsilane as an internal reference and dimethylsulfoxide (DMSO) as a solvent. The hydrodynamic radius, R_h, of the SiO_2 sol was measured using a dynamic laser light scattering (DLLS) ALV500E (Germany). The transmission electron microscope (TEM) micrographs were obtained using a Hitachi 7000 Å microscope (Japan) at an acceleration voltage of 150 kV.

The glass transition temperature (T_g) of the photoresists were measured by a Mettler-Toledo DSC822e (Switzerland). The temperature range was from 0 °C to 130 °C at a constant rate of 10 °C min^{-1} under nitrogen flow. T_g of the sample was determined from the thermogram of the second heating cycle. The thermogravimetric analysis (TGA) was performed on a Mettler-Toledo TGA-SDTA851 thermoanalyzer. In each case a 10 mg sample was examined under a N_2 flow rate of 6×10^{-5} m^3 min^{-1} at a heating rate of 10 °C min^{-1} from room temperature to 600 °C.

The parameters of sensitivity ($D_n^{0.5}$) were determined by a UV energy meter (UV int140) and defined as the dose that retains 50% of the original film thickness after development. The linear thermal expansion coefficients before and after T_g were measured by the linear dimensional variation at different temperatures using a thermal mechanical analysis (TMA2940). The samples were heated from 30 °C to 180 °C at a constant rate of 10 °C min^{-1} under nitrogen flow. The scanning electron microscope (SEM) images of the line width and line type of the photoresists were observed by a Hitachi S-4800 instrument (Japan).

2.3. Synthesis of acrylic copolymer G-ACP

Copolymer ACP was prepared by free radical polymerization with St, BA, MMA, HEA and AA in PMA. A mixture of all monomers (St, BA, MMA, HEA and AA were 0.44 mol, 0.32 mol, 0.47 mol, 0.37 mol and 0.31 mol, respectively) were dropped slowly into 130 mL of PMA at 90 °C with AIBN and 2-ME under vigorously stirring. Free-radical polymerization was carried out for 10 h, and AIBN was added every 2 h for twice. The obtained ACP was heated to 105 °C and added with catalytic agent (TPP) and THPA. Acid value was titrated during reaction until the measured value was about 70 mgKOH g^{-1}, then carboxylic grafted copolymer S-ACP was obtained. Then GMA with inhibitor (MEHQ) was added dropwise into the obtained S-ACP system as well as PMA, to make sure that the solid content was 60 wt%. Then the crude product was cooled down to room temperature and precipitated with methanol/water (v/v = 1/1) solution, which gave acrylic prepolymer G-ACP.

2.4. Synthesis of methacrylate modified nano-SiO_2 (SiO_2MA)

The nano-SiO_2 sol was synthesized from TEOS through sol–gel process [26]. A mixture of ethanol (2.34 mol), deionized water (18 mL) and $NH_3{\cdot}H_2O$ (0.01 mol) was stirred vigorously at 50 °C, and dropped with TEOS (0.13 mol) in 1 h. The reaction was maintained at 50 °C for 24 h, resulting in a nano-SiO_2 sol. At the same time, 0.18 mol of GMA was dropped into 0.09 mol of KH550 at 75 °C with vigorously stirring. After 7 h reaction, the precursor KHMA was obtained. Then all of KHMA was dropped into 100 g of obtained nano-SiO_2 sol and stirred at 50 °C for 24 h. The crude product was mixed with PMA and vacuum distilled at 30 °C for 1 h to remove the residuals (e.g., ethanol, water and $NH_3{\cdot}H_2O$), obtaining transparent methacrylate modified SiO_2MA.

2.5. Preparation of cured organic–inorganic nanocomposites photoresists

The primary photoresist formula utilized in this study was a 10:1 mixture of G-ACP to TPGDA in weight, added with photoinitiator and photosensitizer (6 wt%, Irgacure 907/ITX = 2) and inhibitor HQ (0.5 wt%). Then SiO_2MA was added into the primary photoresist formula with the concentration of 3.8, 7.3, 10.6 and 13.7 wt%, which are denoted as NCP-1, NCP-2, NCP-3 and NCP-4, respectively.

The prepared nanocomposite photoresists were uniformly spread on a preprocessed copper-clad plate with a bar-spreader (15 μm) and pre-baked at 75 °C for 30 min until the films were dried. Then all the sample plates were placed in an exposure box for 30 s, in which a UV mercury lamp of 1000 W with a main wavelength of 365 nm was situated at a distance of 15 cm from the sample plates. After UV exposure, the sample plates were immersed in sodium carbonate solution (1 wt%, 33 °C ± 2 °C) for 60 s for development. For comparison, the primary photoresist

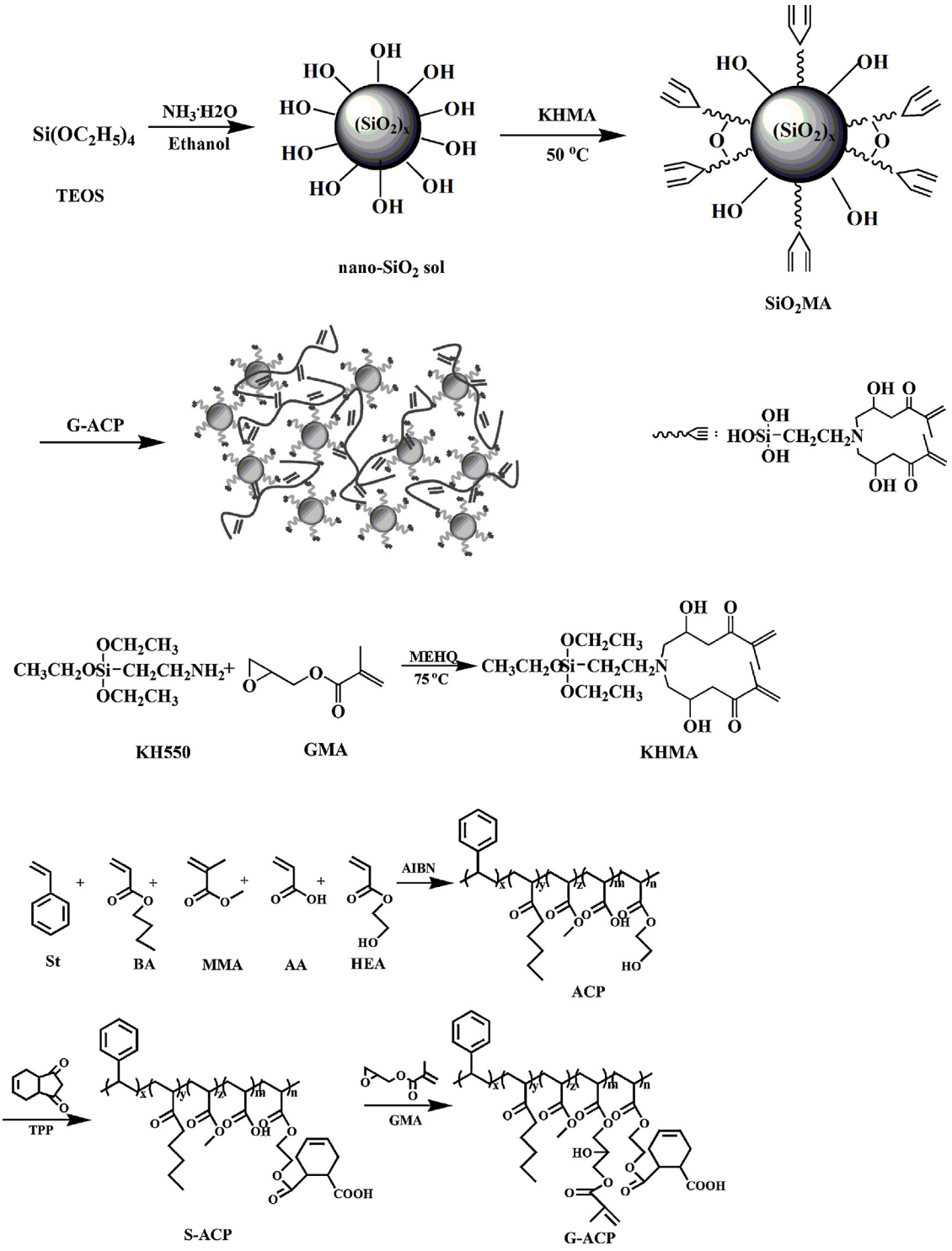

Scheme 1. Preparation route and structural illustration of KHMA, G-ACP and cured organic–inorganic nanocomposites photoresists.

underwent all the exposure-development procedure and named as NCP-0. The illustrated diagram for preparing the organic–inorganic nanocomposite photoresists is shown in Scheme 1.

3. Results and discussion

3.1. Preparation and characterization of ACP, S-ACP and G-ACP

FT-IR and ^{1}H NMR measurements were performed to determine the molecular structures of ACP, S-ACP and G-ACP. Fig. 1 illustrates the FT-IR spectra of ACP, S-ACP and G-ACP. The absorption peak at 3480 cm^{-1} is attributed to the O–H stretching vibration from carboxyl group and hydroxyl group. The broad absorption peak from 3500 cm^{-1} to 2500 cm^{-1} is assigned to the stretching vibration of hydrogen bond. Characteristic peak at 1735 cm^{-1} arises from the C=O stretching vibration of carbonyl and ester groups, and absorption peak at 762 and 702 cm^{-1} are assigned to the bending vibrations of phenyl ring, respectively. These peaks observed from the curve of ACP demonstrated the successful copolymerization of five monomers (St, BA, MMA, HEA and AA).

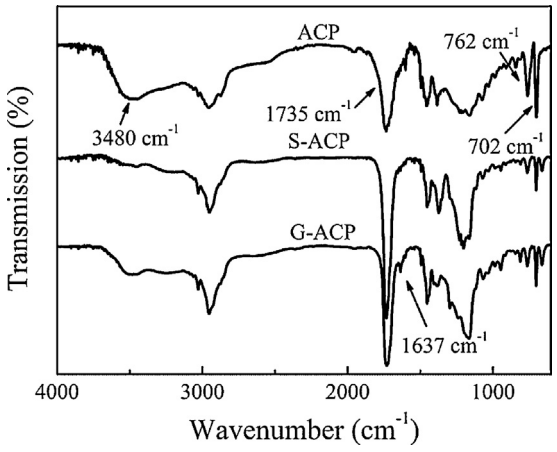

Fig. 1. FT-IR spectra of ACP, S-ACP and G-ACP.

Moreover, the same characteristic peaks occur in the spectrum of S-ACP as that of ACP except that the absorption peak at 3480 cm^{-1} is weakened, which indicates that THPA was successfully grafted to ACP via the reaction between hydroxyl and anhydride group. Besides, an absorption peak at 1637 cm^{-1} assigned to the stretching band of C=C is observed from the G-ACP spectrum. This indicates that GMA was grafted to S-ACP through the reaction between epoxy and carboxyl group, and acrylic copolymer G-ACP was successfully synthesized.

The ^{1}H NMR spectra of ACP and G-ACP are shown in Fig. 2. The characteristic peaks for ACP are clearly seen at 0.8–1.0 ($-CH_3$), 3.7 ($-CH_2OH$), 4.0 ($-OCH_2-$, $-OCH_3$), 4.7 ($-CH_2CH(COO)-$, $-CH_2CHC_6H_5-$), 6.8–7.2 ($-C_6H_5$), 12.1 (–COOH) ppm. In the spectrum of G-ACP, a new peak is represented at 5.8–6.1 ppm for CH_2=C– introduced by GMA and THPA.

3.2. Preparation and characterization of KHMA, nano-SiO_2 and SiO_2MA

The acrylic precursor KHMA was prepared through the reaction between GMA and KH550. Fig. 3 shows the FT-IR spectra of GMA and KHMA. The characteristic peaks at 1254 and 912 cm^{-1} attributed to the stretching vibration of epoxy group are observed in the curve of GMA, as well as the absorption peaks at 1638 and 810 cm^{-1} for the C=C stretching and bending vibration,

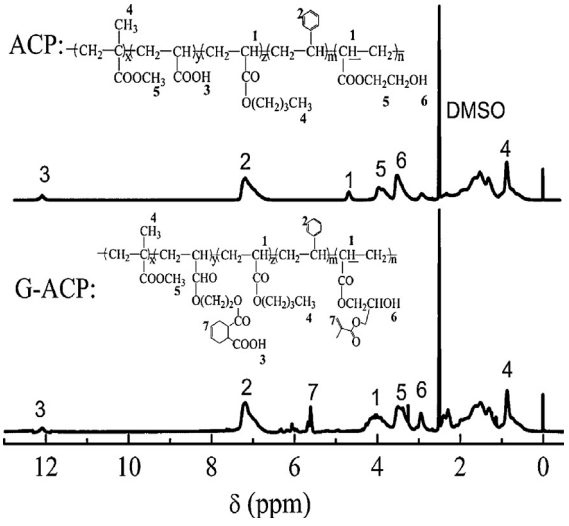

Fig. 2. ^{1}H NMR spectra of ACP and G-ACP.

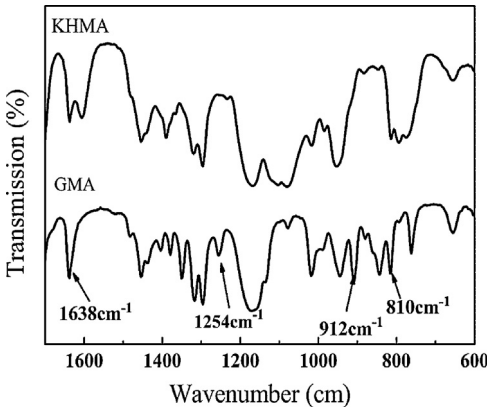

Fig. 3. FT-IR spectra of GMA and KHMA.

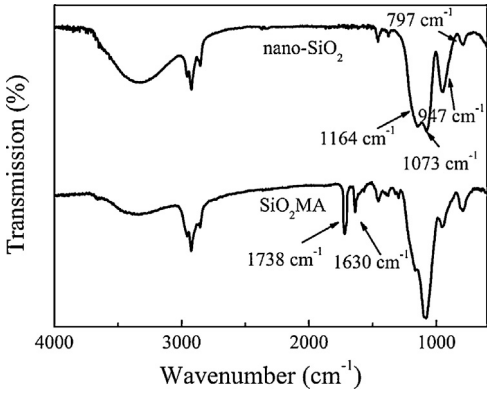

Fig. 4. FT-IR spectra of nano-SiO_2 and SiO_2MA.

respectively. However, the disappearance of the absorption peaks at 1254 and 912 cm^{-1} in the curve of KHMA demonstrates the successfully reaction between epoxy group of GMA and amino group of KH550. Moreover, new peaks at 1638 and 810 cm^{-1} for the C=C group appear in the curve of KHMA. Both of them indicate the successful synthesis of KHMA.

The nano-SiO_2 and SiO_2MA are obtained by a sol–gel process and the FT-IR spectra of them are represented in Fig. 4. For the nano-SiO_2, the broad adsorption peak from 3600 and 3000 cm^{-1} is assigned to O–H stretching vibration. Besides, the characteristic peaks at 1073 and 797 cm^{-1} represent the stretching vibrations of

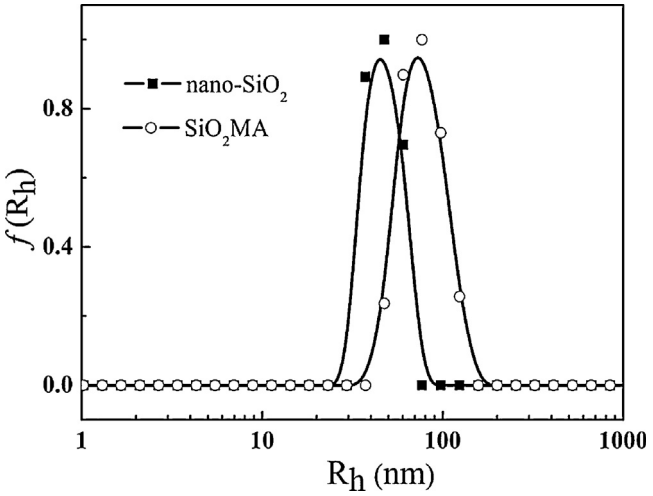

Fig. 5. The R_h of nano-SiO_2 and SiO_2MA measured by DLLS.

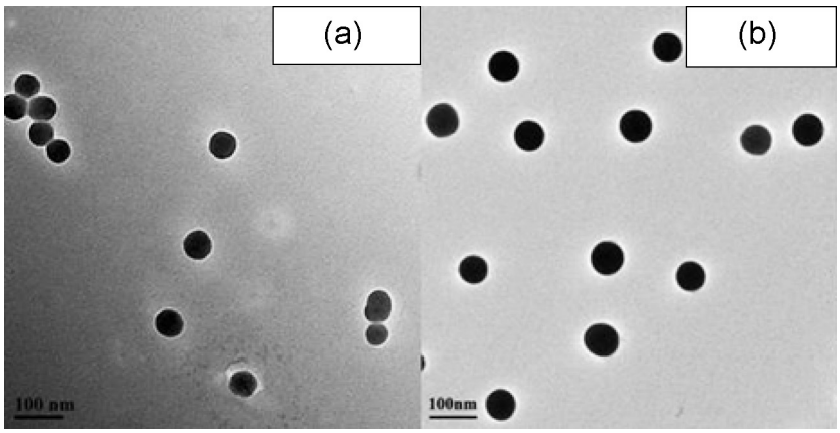

Fig. 6. TEM micrographs of nano-SiO_2 (a) and SiO_2MA (b) dispersed in PMA solution.

the Si–O–Si bond and the peak at 1164 cm^{-1} is attributed to the stretching vibration of the Si–O–C, respectively. The adsorption band at 947 cm^{-1} is assigned to the Si–OH. However, the weakening of the broad adsorption peak from 3600 and 3000 cm^{-1} and the appearance of new absorption peaks at 1738 and 1630 cm^{-1} associated with C=C and C=O in the curve of SiO_2MA both indicates that the SiO_2MA modified with methacrylate was successfully prepared through the hydrolysis and condensation of KHMA with nano-SiO_2.

The particle sizes of the nano-SiO_2 and SiO_2MA, shown in Fig. 5, are analyzed with DLLS by measuring R_h. It shows that the particle size of SiO_2MA (Fig. 5b) is about 74 nm, which is larger than the size of the nano-SiO_2 (Fig. 5a) at 45 nm. For visual observation of the morphology of nano-SiO_2 and SiO_2MA, the TEM micrographs of the PMA solution of nano-SiO_2 and SiO_2MA were taken and shown in Fig. 6. The SiO_2MA (Fig. 6b) reveals a larger particle size and better dispersion compared to nano-SiO_2 (Fig. 6a). This can be explained that there are a lot of organic chains grafted to the surface of SiO_2MA, which improved the dispersion of SiO_2MA in organic solutions.

3.3. Photosensitivity of organic–inorganic nanocomposite photoresists

The photosensitivity of organic–inorganic nanocomposite photoresists was measured by the parameter of sensitivity ($D_n^{0.5}$), defined as the dose that retains 50% of the original film thickness after development. Fig. 7 represents the curves of all nanocomposite photoresists and the primary photoresist for exposure doses ranging from 0 to 130 mJ cm^{-2}. The $D_n^{0.5}$ of NCP-0 for the primary photoresist is 52.4 mJ cm^{-2} while the $D_n^{0.5}$s of nanocomposite photoresists are 48.6, 39.2, 29.3 and 26.8 mJ cm^{-2} for NCP-1 to NCP-4, respectively. Obviously, the $D_n^{0.5}$ decreases with increasing the content of SiO_2MA, which indicates a better photosensitivity with the addition of SiO_2MA modified with methacrylate. This can be explained by the migration of nano silica onto surface due to their low surface energy and therefore the enrichment of SiO_2MA at the surface of nanocomposite photoresists. Moreover, G-ACP can form hydrogen bond with SiO_2MA between the hydroxyl group in the side chain of G-ACP and Si–O bonds of SiO_2MA, which leaves the enrichment of G-ACP together with SiO_2MA at the surface of nanocomposite photoresists. Therefore, a high concentration of double bonds on the surface of nanocomposite photoresists from methacrylate groups in both G-ACP and SiO_2MA brings a great improvement of photosensitivity for the nanocomposite photoresists.

3.4. Thermal properties of cured organic–inorganic nanocomposite photoresists

Fig. 8 shows the thermograms of nanocomposite photoresists and the primary photoresist measured by differential scanning calorimeter (DSC). T_g of the nanocomposite photoresists was determined from the thermogram in the second heating cycle. It appears that T_g of nanocomposite photoresists increases as the increase of SiO_2MA content and the detail data are shown in Fig. 8. It is well-known that the restriction of the macromolecular chain

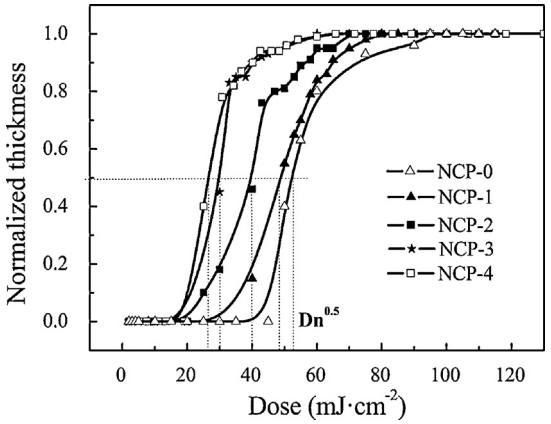

Fig. 7. Characteristic curves of nanocomposites photoresists with different SiO_2MA loading (wt%): NCP-0 (0%), NCP-1 (3.8%), NCP-2 (7.3%), NCP-3 (10.6%) and NCP-4 (13.7%).

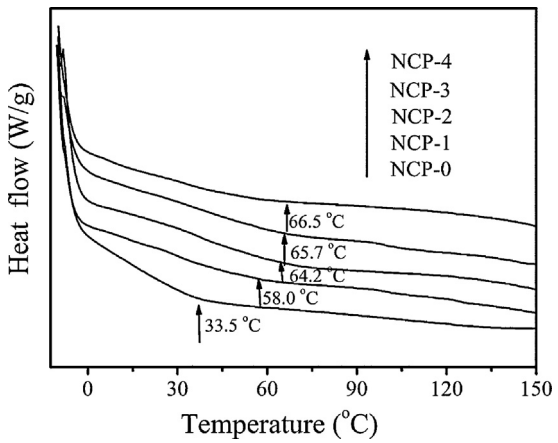

Fig. 8. DSC thermograms of cured primary photoresist and nanocomposites photoresists.

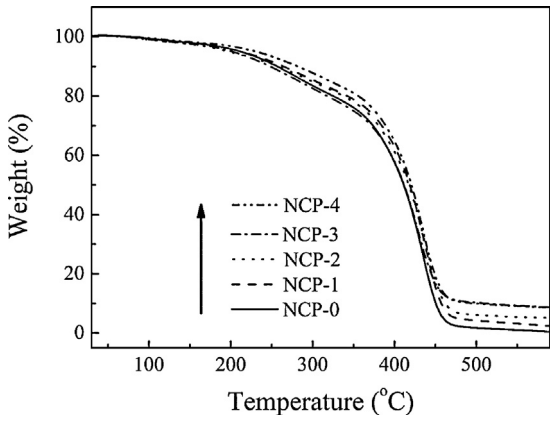

Fig. 9. TGA curves of cured primary photoresist and nanocomposites photoresists.

motion would make the requisite thermal energy for the occurrence of glass transition higher. In this case, the hydrogen bonding interaction between Si–O–Si of SiO_2MA and the hydroxyl group of G-ACP restricts the segmental motion near the organic–inorganic interface, leading to a higher temperature to achieve the transition.

The TGA curves of cured nanocomposite photoresists in comparison with that of the primary photoresist are shown in Fig. 9. It is shown that the thermal decomposition performance of all nanocomposite photoresists is similar with the primary photoresist except for the raised onset decomposition temperature as the SiO_2MA loading increases. The temperature of 5% mass loss is defined as the onset decomposition temperature (T_d) and the T_d of NCP-0 to NCP -4 are determined as 196, 203, 209, 211 and 230 °C, respectively. Besides, the char residues display the same trend with 0.4%, 2.2%, 5.0%, 8.5% and 8.7% for NCP-0, NCP-1, NCP-2, NCP-3 and NCP-4, respectively. Both of them demonstrate the enhancement of thermal stability with the addition of SiO_2MA. This can be explained by the high bond dissociation energy of Si–O–Si bond and the high double bond concentration brought by SiO_2MA.

The linear thermal expansion coefficient (α) is a very important factor for photoresists because the tiny deformation would cause a huge impact on the last circuit image. The thermal expansion coefficients before (α_1) and after (α_2) glass transition of nanocomposite photoresists and the primary photoresist were measured using TMA and the detail results are listed in Table 1. The primary photoresist without SiO_2MA has high α_1 and α_2 of 100.0 and 118.5 μm (m °C)$^{-1}$ due to the intrinsic property of polymers. Both α_1 and α_2 decrease with the increase of SiO_2MA content. Especially, α_1 and α_2 of NCP-4 with 13.7 wt% SiO_2MA addition have

Table 1
Coefficients of thermal expansion of cured primary photoresist and nanocomposites photoresists.

Sample	α_1 (μm(m °C)$^{-1}$)	α_2 (μm(m °C)$^{-1}$)
NCP-0	100.0	118.5
NCP-1	95.7	114.3
NCP-2	92.6	108.8
NCP-3	83.4	93.7
NCP-4	75.6	87.4

Table 2
Adhesion, pencil hardness, solvent resistance and resolution of cured primary photoresist and nanocomposites photoresists.

Sample	Adhesion	Pencil hardness	Solvent resistance (MEK)	Resolution (μm)
NCP-0	100	2H	>60	<25
NCP-1	100	3H	>64	<25
NCP-2	100	3H	>72	<25
NCP-3	100	4H	>85	<25
NCP-4	100	4H	>90	<25

great decrease of 25 and 30 μm (m °C)$^{-1}$ compared to NCP-0, considered as great improvement of pure polymer. This could be attributed to the incompressible property of silica and the higher double bond density due to SiO_2MA, therefore it results in the good dimensional stability of nanocomposite photoresists.

3.5. Adhesion, hardness, solvent resistance and resolution of cured organic–inorganic nanocomposite photoresists films

The adhesion strength of nanocomposite photoresists and the primary photoresist film coated on tinplate substrate was examined by the tape test, meanwhile the hardness was determined using the pencil test. The tested results are listed in Table 2 as well as the MEK resistance times. All photoresists show perfect adhesion on the tape test while the pencil hardness improves with increasing of the SiO_2MA content. The same result was observed for the MEK resistance, all due to the high cross-linking density and the stiffness of silica from SiO_2MA.

Finally, the resolution of photoresists was observed through optical microscopic images of the patterns prepared by the nanocomposite photoresist NCP-3 and the primary photoresist. And the images are shown in Fig. 10. Both of them have a good linear pattern of less than 25 μm. It avoids the reduction of developing ability induced by incorporation of inorganic nanocomposites into photoresists. This can be attributed to the methacrylate group grafted on SiO_2MA, which improves the cross-linking density as well as the photopolymerization ability.

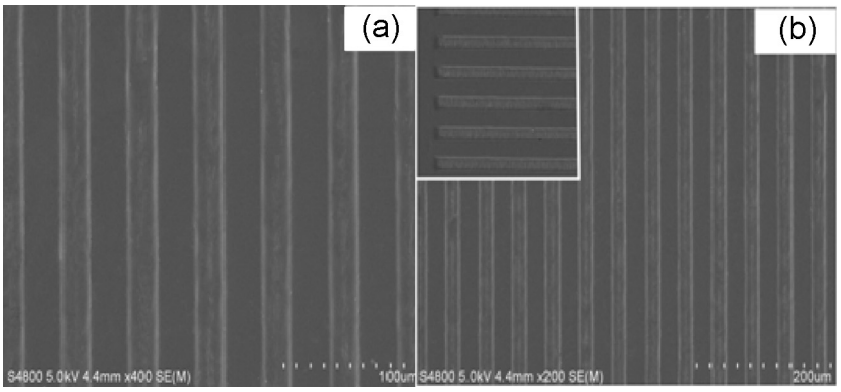

Fig. 10. Optical microscopic images of the patterns formed using nanocomposites photoresist NCP-3 (a) and the primary photoresist (b).

4. Conclusion

A novel nano-SiO_2 modified with methacrylate was synthesized and incorporated into an acrylic copolymer, thus a series of UV-cured organic–inorganic photoresists via a standard thermal and UV-exposure process were prepared. The photosensitivity was greatly enhanced with the addition of SiO_2MA, due to the high concentration of double bond in the surface of nanocomposite photoresists caused by SiO_2MA. Moreover, the thermal and mechanical properties, and resolution were enhanced as well.

Acknowledgements

This work was supported by the National Nature Science Foundation of China (No. 51203063 and 51003041), the National Nature Science Foundation of Jiangsu Province (No. BK20130153) and the Fundamental Research Funds for the Central Universities (No. JUSRP1021).

References

[1] H.Z. Xi, Q. Liu, S.M. Guo, Mater. Lett. 80 (2012) 72–74.
[2] M.D. Ynsa, P. Shao, S.R. Kulkarni, N.N. Liu, J.A. van Kan, Nucl. Instrum. Methods B 269 (2011) 2409–2412.
[3] Y.Y. Liao, J.H. Liu, J. Appl. Polym. Sci. 109 (2008) 3849–3858.
[4] H. Chen, J. Yin, J. Polym. Sci. Part A: Polym. Chem. 42 (2004) 1735–1744.
[5] Y. Watanabe, K.I. Fukukawa, Y. Shibasaki, M. Ueda, J. Polym. Sci. Part A: Polym. Chem. 43 (2005) 593–599.
[6] D.M. Ornoff, Y. Wang, N.L. Allbritton, J. Micromech. Microeng. 23 (2013) 1543–1551.
[7] C.T. Chen, C.T. Chuang, Micro Nano Lett. 7 (2012) 733–735.
[8] J.S. Lee, S.I. Hong, Eur. Polym. J. 38 (2002) 387–392.
[9] S.C. Kim, D.H. Nam, Y.H. Kim, B.K. Song, Biotechnol. Bioproc. Eng. 15 (2010) 208–212.
[10] S.W. Zhang, A.X. Yu, S.L. Liu, J. Zhao, J.Q. Jiang, X.Y. Liu, Polym. Bull. 68 (2012) 1469–1482.
[11] M. Lillemose, L. Gammelgaard, J. Richter, E.V. Thomsen, A. Boisen, Compos. Sci. Technol. 68 (2008) 1831–1836.
[12] J. Jakobi, S. Petersen, A. Menendez-Manjon, P. Wagener, S. Barcikowski, Langmuir 26 (2010) 6892–6897.
[13] S. Jiguet, M. Judelewicz, S. Mischler, A. Bertch, P. Renaud, Microelectron. Eng. 83 (2006) 1273–1276.
[14] S.S.C. Yu, A.J. Downard, Langmuir 23 (2008) 4662–4668.
[15] S. Jiguet, A. Bertsch, M. Judelewicz, H. Hofmann, P. Renaud, Microelectron. Eng. 83 (2006) 1966–1970.
[16] H.M. Lin, S.Y. Wu, P.Y. Huang, C.F. Huang, S.W. Kuo, F.C. Chang, Macromol. Rapid Commun. 27 (2006) 1550–1555.
[17] H.M. Lin, K.H. Hseih, F.C. Chang, Microelectron. Eng. 85 (2008) 1624–1628.
[18] D. Eon, G. Cartry, V. Fernandez, C. Cardinaud, E. Tegou, V. Bellas, P. Argitis, E. Gogolides, J. Vac. Sci. Technol. B 22 (2004) 2526–2532.
[19] Y.N. Duan, S.C. Jana, A.M. Reinsel, B. Lama, M.P. Espe, Langmuir 28 (2012) 15362–15371.
[20] X.E. Cheng, S.Y. Liu, W.F. Shi, Prog. Org. Coat. 65 (2009) 1–9.
[21] I.E. dell'Erba, R.J.J. Williams, Eur. Polym. J. 43 (2007) 2759–2767.
[22] H. Mori, Y. Miyamura, T. Endo, Langmuir 23 (2007) 9014–9023.
[23] P. Hajji, L. David, J.F. Gerard, J.P. Pascault, G. Vigier, J. Polym. Sci. Polym. Phys. 37 (1999) 3172–3187.
[24] G. Bonilla, M. Martinez, A.M. Mendoza, J.M. Widmaier, Eur. Polym. J. 42 (2006) 2977–2986.
[25] C.K. Lee, T.M. Don, W.C. Lai, C.C. Chen, D.J. Lin, L.P. Cheng, Thin Solid Films 516 (2008) 8399–8407.
[26] D.J. Lin, T.M. Don, C.C. Chen, B.Y. Lin, C.K. Lee, L.P. Cheng, J. Appl. Polym. Sci. 107 (2008) 1179–1188.
[27] J.D. Cho, H.T. Ju, Y.S. Park, J.W. Hong, Macromol. Mater. Eng. 291 (2006) 1155–1163.